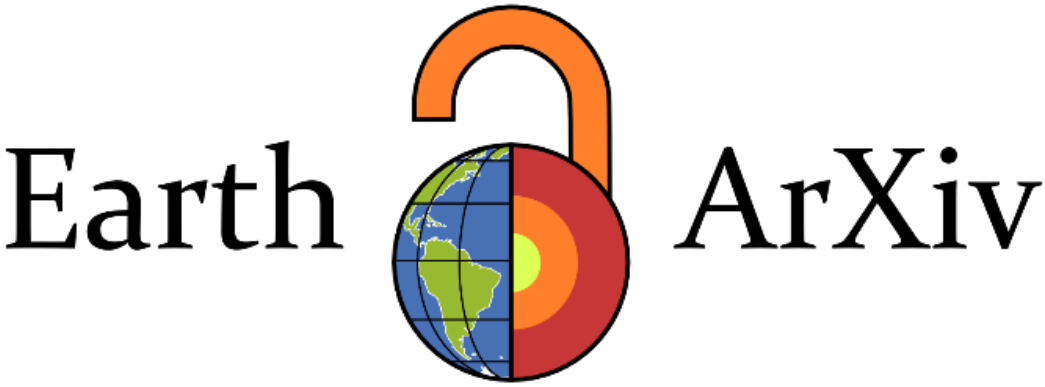

Please send any comments, feedback, or suggestions to benjamin.hatchett@colostate.edu

Visualizing Pyroclimatology

Benjamin J. Hatchett[1,2*], T. Todd Lindley[3], John T. Abatzoglou[4], Ansley Baring[5], Alexander Gershunov[6], Kristen Guirguis[6], Robert Munroe[7], Nick J. Nauslar[8], Eli Orland[9], Alan M. Rhoades[10], Karen Short[11], Rochelle P. Worsnop[12]

[1*]Cooperative Institute for Research in the Atmosphere, Colorado State University, 4000 West Laporte Avenue, Fort Collins, 100190, CO, USA.
[2]Affilate working on a cooperative grant with the NOAA/Global Systems Laboratory, 325 Broadway, Boulder, 80305, CO, USA.
[3]National Weather Service, Norman, 120 David L. Boren Blvd. Suite 2400, Norman, 73072, OK, USA.
[4]Management of Complex Systems, School of Engineering, University of California, Merced, West Laporte Avenue, Merced, 100190, CO, USA.
[5]NOAA/Global Systems Laboratory, 325 Broadway, Boulder, 80305, CO, USA.
[6]Scripps Institution of Oceanography, University of California, San Diego, 8622 Kennel Way, La Jolla, 92037, CA, USA.
[7]National Weather Service, Los Angeles, 520 North Elevar St., Oxnard, 93030, CA, USA.
[8]NOAA/Storm Prediction Center, 3833 Development Ave, Boise, 83705, ID, USA.
[9]NASA Goddard Space Flight Center/University of Maryland, Baltimore County, Mail Code 618, Greenbelt, 20771, MD, USA.
[10]Lawrence Berkeley National Laboratory, 1 Cyclotron Rd., Berkeley, 94720, CA, USA.
[11]Rocky Mountain Research Station, United States Forest Service, 240 West Prospect Rd., Fort Collins, 80526, MT, USA.
[12]NOAA/Physical Sciences Laboratory, 325 Broadway, Boulder, 80305, CO, USA.

*Corresponding author(s). E-mail(s): benjamin.hatchett@gmail.com;

Abstract

Background: Wildland fire activity often demonstrates distinct seasonality adhering to the alignment of climatologically favorable fuels, weather, and ignitions for wildfire or prescribed burning. Improved characterization of conditions that increase fire ignition probabilities, extreme fire behavior, and beneficial fire potential would enhance our understanding of fire regimes and provide insight for future wildland fire management.

Methods: We apply a commonly-utilized tool–the climograph–to visually communicate historical wildland fire activity by demonstrating fire seasonality, interannual variability, and past individual fire events at daily resolution using satellite observations to three distinct fire-prone and fire-requiring areas.

Results: Detection counts and cumulative fire radiative power in the resulting pyroclimographs provide first-order indicators of changes in fire activity occurring within- and out-of-season for the fire type (i.e., wildfires or prescribed burns). Using a case study of coastal Southern California, we show how pyroclimographs vary as the region of interest shifts and how their interpretation can be complemented by including climatological interpretations of additional fire environment data. Pyroclimographs also help characterize the fraction of fire radiative power–a proxy for emissions and burn severity–contributed from few or many events, i.e., the number of days contributing 50% or 90% of total fire radiative power since satellite observations began.

Conclusions: Information contained within a pyroclimograph may help track current conditions, identify factors associated with past fire occurrence, or understand typical timing of smoke impacts and their sources, all of which can be interpreted in the context of evolving real-time conditions and used for longer-term planning. Given the current ubiquity and projected increase of wildland fire in many regions, we recommend considering pyroclimographs as a visualization tool supporting varied applications where information regarding wildland fire seasonality and characteristics will benefit users.

Keywords: climatology, fire history, fire weather, remote sensing, visualization

1 Introduction

Climographs convey a region's climatic seasonal cycle by displaying the monthly mean temperature range and total precipitation (e.g., Lasantha et al. 2022; Al-Yaari et al. 2023). Many regions also demonstrate a seasonal cycle of fire activity resulting from the annual march of plant phenology–a growing season when fuel accumulates and a dormant season when fuel becomes available for combustion–and the interplay of prolonged and short-term weather conditions. Fire events resulting from natural and human ignitions are are linked by climate and punctuated by weather including the evolution of precipitation, temperature, snowpack, heat waves, humidity, and winds.

Visually linking the seasonality of environmental conditions to the cycle of fire danger for situational awareness has literally been in the pocket of firefighters as a 'pocket card' for over 20 years (Schlobohm 2000). The term 'pyroclimograph' arose from the juxtaposition of monthly mean temperature and precipitation with monthly

burned area (Swetnam et al. 2011). Sablan et al. (2024) developed similar visualizations of monthly fire activity to show the top 10^{th} and bottom 10^{th} percentiles and mean of a historical record as well as highlight a particular year of interest. Sweeney et al. (2025) generated weekly-timescale visualizations and separated prescribed burns (i.e., pile and broadcast) from wildfires to show the distinct seasonalities of wildland fire types.

However, many wildland fires, especially prescribed burns (Hatchett and Wells 2026) or damaging fast fires (Hantson et al. 2022; Balch et al. 2024) burn only for hours or a few days, rendering aggregation to monthly or even weekly timescales potentially misleading. These short timescales of burn periods may occur during periods of increased fuel receptiveness amidst varied background environmental states, implying a climatological perspective also requires consideration of weather. During briefly intensified fire activity, temporal aggregation limits our interpretation of how anomalous the environmental conditions were compared to climatology. Understanding the conditions leading to increased receptiveness of fuels and the potential for extreme fire behavior may support fire management and community adaptation efforts at annual to decadal timescales as well as characterizing a region's general fire environment. This is important for safely and effectively conducting prescribed burning (Worsnop et al. 2026), a necessary component for achieving wildfire resiliency and restoring ecosystem function in fire-dependent regions. Further, understanding fire seasonality may inform ideal times to promote campaigns for smoke-ready communities and other community fire prevention, mitigation, and preparedness efforts.

Over two decades of satellite-based fire detections at subdaily timescales make it possible to produce climatologies of fire activity at daily resolution for a user-defined region. Regions can reflect operational needs or efforts supporting emergency and resilience planning. For example, a region could be jurisdictionally defined, such as a county or National Weather Service (NWS) County Warning Area (CWA). It could also be physically-defined such as a watershed, ecoregion (Omernik and Griffith 2014), mountain range (Snethlage et al. 2022), or pyrome (Short et al. 2020). Ultimately, the goal is to provide a flexible capability–a regionally-relevant pyroclimograph at daily resolution–for visualizing environmental conditions associated with past fire activity and the timing of varied fire types (e.g., prescribed burns and wildfire). Decision support opportunities include operational fire management, prescribed burn planning, community messaging for wildfire prevention and preparedness, smoke readiness, long-term adaptation and mitigation efforts for hazard reduction, or research activities to better understand conditions supporting varied fire ignition and behavior patterns.

This brief report provides four examples of the construction and interpretation of pyroclimographs utilizing fire detection data to gain insights about fire activity in three fire-prone landscapes. First, we construct pyroclimographs to illustrate fire activity in Colusa County, California, a region with distinct wildfire and prescribed burning seasonality. Second, we show how pyroclimographs can document the near-real-time progression of a fire season in the U.S. Southern Great Plains. Third, we show how results, particularly seasonality, vary across different geographic delineations in coastal Southern California. Fourth, we demonstrate how a more complete pyroclimograph will incorporate ancillary fire environment data.

2 Data

We used satellite fire detections from the Moderate Resolution Imaging Spectroradiometer (MODIS) onboard the Terra and Aqua spacecraft (Giglio et al. 2016) and acquired from the NASA Fire Information for Resource Management System (https://firms.modaps.eosdis.nasa.gov/) for the period spanning 1 January 2001 to 1 April 2026. County shapefiles were acquired from the U.S. Census Bureau (https://www2.census.gov/geo/tiger/TIGER2025/COUNTY/). Shapefiles for the NWS CWAs were acquired from the NWS County Warning Boundary Area Dataset (https://www.weather.gov/gis/CWABounds). The Southern California Mountains/Northern Baja pyrome was extracted from (Short et al. 2020). Environmental Protection Agency (EPA) Level 3 ecoregions (Omernik and Griffith 2014) were acquired from https://www.epa.gov/eco-research/level-iii-and-iv-ecoregions-continental-united-states. Last, we used a boundary delineating the Santa Monica Mountains, a subset of the Transverse Ranges and excluding the Palos Verdes Hills, from the Global Mountain Biodiversity Assessment Mountain Inventory version 2.0 (Snethlage et al. 2022).

To more fully characterize the fire environment, we used hourly observations of 2-m air temperature, 2-m relative humidity and 6-m (∼20 ft) wind speed from the Malibu Hills, California Remote Automatic Weather Station (RAWS; acquired from the Western Regional Climate Center at: https://raws.dri.edu) for the station's period-of-record (January 1995–February 2026) to capture the spread component. Daily, gridded ∼4 km horizontal resolution estimates of energy release component spanning 1979–2025 were acquired from the gridMET product (Abatzoglou 2013) to capture the ignition component.

3 Methods

Analysis of fire detection latitude, longitude, fire radiative power (FRP), and time of detection, as well as other fire environment data, was performed using Matlab (The MathWorks Inc. 2024). Desiring maximum detectability, we did not omit detections based on confidence values, which may include anomalous detections due to industry or sun glint. For each calendar day across all years, the total number of detections are counted and reported by a bar chart (Figures 1b,d); specific years of interest can be plotted separately. Similarly, cumulative FRP across each calendar day in the period-of-record is calculated to show seasonality of fire activity (right hand y-axis of Figures 1b and d). Lastly, we calculate the total FRP over the period of record and then sort the daily FRP entries in descending order to determine the number of days that it took to reach the 50%, 75%, and 90% of the total FPR (text beneath Figures 1b,d). While 1 January was selected as the starting point, depending on user needs, much like water years, the 'fire year' could be expressed as a 'wind year' that orients the peak windy season in the center of the figure.

To show the seasonality of fire danger in the Santa Monica Mountains example (Figure 3), gridMET-based estimates of energy release component (ERC) were extracted for a box encompassing the region (Figure 3b). The 3^{rd}, 5^{th}, 20^{th}, 50^{th}, 80^{th}, and 97^{th} percentiles were calculated between 1979–2025 at a daily scale (plotted

with 5 day running mean to smooth the data). The 3^{rd}, 50^{th}, and 97^{th} percentiles were calculated across all days.

Last, fire weather hours were estimated using the available summed daily number of hours between 1995–2024 meeting either set of criteria for a Red Flag Warning at the NWS Fire Weather Zones (FWZ) 369 and 370 (California Annual Operating Plan 2025): 1) relative humidity $\leq 10\%$ with sustained wind speed $\geq 6.7\ m\ s^{-1}$ ($\geq 15\ miles\ hr^{-1}$) or gusts $\geq 11.2\ m\ s^{-1}$ ($\geq 25\ miles\ hr^{-1}$) or 2) relative humidity $\leq 15\%$ with sustained wind speed $\geq 11.2\ m\ s^{-1}$ ($\geq 25\ miles\ hr^{-1}$) or gusts $\geq 15.6\ m\ s^{-1}$ ($\geq 35\ miles\ hr^{-1}$). If these conditions are sustained for $> 6hr$ with critically dry fuels, a Red Flag Warning may be issued. Under certain extreme conditions, forecasters will coordinate with fire agencies to relax constraints for Red Flag Warning issuance.

4 Results

4.1 Pyroclimographs: A Simple Interpretation and Application

Colusa County, CA–an agricultural community–demonstrates three distinct burn seasons as evidenced by small increases in annual accumulations of FRP during late winter to early spring (mid-January–April), a more rapid increase during the extended summer (late June–September), and a shift back to gradual but annually consistent increases during fall (October–November; Figure 1a). Following the regional prescribed burn climatology produced by Worsnop et al. (2026) and examining wildfire history data hosted by CAL FIRE (https://www.fire.ca.gov/what-we-do/fire-resource-assessment-program; not shown), we interpret the consistent daily detections (Figure 1b) with lower FRP as indicating the seasonal nature of planned agricultural burning and prescribed burning of wildlands during spring and fall, while more brief instances of higher FRP indicate named summer wildfire incidents (e.g., 2012, 2018, and 2024). Incorporating additional agency (or other) records of prescribed burns versus wildfire events is recommended to differentiate the seasonality of fire types.

Wildfire and prescribed fire occur in the U.S. Southern Great Plains throughout the year, though a peak in fire activity occurs in February following the dry winter season and terminates with the onset of the spring convective season in April (Figure 1c–d). As fire detection data is made publicly available on the order of hours after a satellite overflight, pyroclimographs can be used to track the progression of a fire season in near-real-time. With persistent drought and heavy fine fuel loading priming the fire environment, a dry and windy spring initiated the 2026 wildfire season approximately two weeks early based on the available climatological data record (red line in Figure 1c). While the annual cumulative curves (Figures 1a and 1c) allow the comparison of years against one another–for example, to identify early onset of fire activity–for the remainder of the manuscript, we focus on the detection bar charts (Figure 1b and 1d).

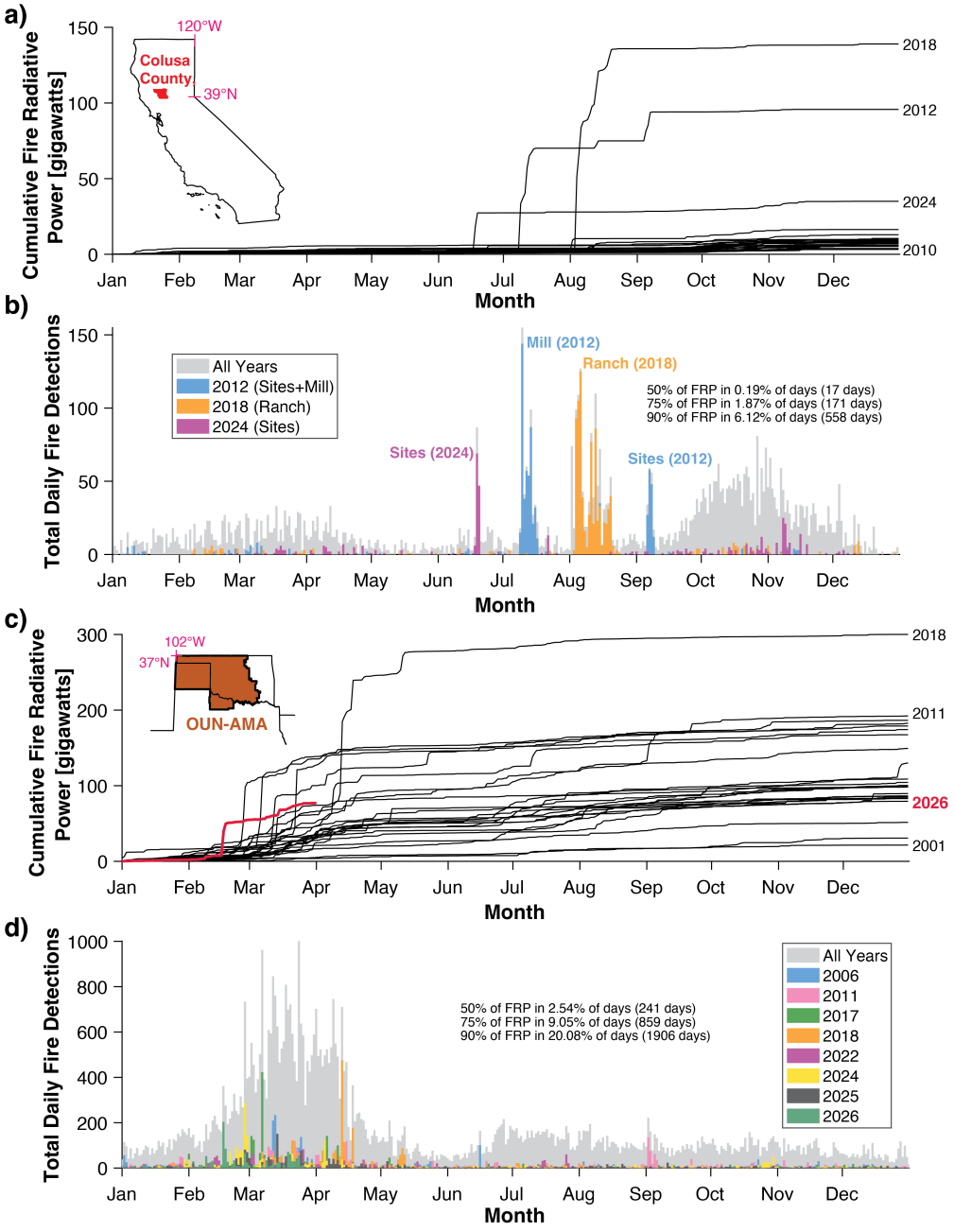

Fig. 1 (a) Pyroclimograph showing daily cumulative fire radiative power for each calendar year (2001–2025; highest three and lowest year shown) for Colusa County, California. (b) Period-of-record total daily fire detections across years (gray bars). Contributions from notable fires are colored. (c–d) As in (a–b) but for the Norman, Oklahoma (OUN) and Amarillo, Texas (AMA) NWS CWAs (2026 shown in bold red).

4.2 Variability across coastal Southern California

Coastal Southern California is a densely populated, fire-prone but ignition-limited landscape with extraordinary exposure of values-at-risk to wildland fire. Here, we explore how pyroclimographs contribute to fire history interpretation across different domains within this larger region. Starting at the largest scale, the Southern California Mountains/Northern Baja pyrome spans interior Santa Barbara County to San Diego County (Figure 2a). This large region has experienced many notable wildfires between May and early January, but also shows evidence of cool season prescribed burning (consistent but few detections). Two EPA Level 3 Ecoregions comprise the pyrome. In the mid-to-higher elevation, conifer-dominated Southern California Mountains ecoregion, fire season typically spans June to mid-October but can include anomalous dry downslope Santa Ana wind-driven fire events such as the late October firestorms in 2003 and 2007 as well as the December 2017 Thomas Fire and January 2025 Los Angeles Palisades and Eaton Fires (Figure 2b). The lower elevation, chaparral and coast sage and chaparral-dominated Southern California Coast/Northern Baja ecoregion has fewer fires in the summer (one exception being the 2018 Holy Fire), owing to cool and moist marine layer influences (Figure 2c). Wildfires are most common in late fall and into winter if Santa Ana winds begin before season-ending precipitation occurs in October or November (Cayan et al. 2022).

The NWS Los Angeles CWA (Figure 2d) includes more interior dry regions and elevated terrain susceptible to human and lightning ignitions that yield a longer overall fire season from May through early January with a notable peak in activity between July and September. Similar to the coastal regions, delayed winter precipitation exposes the region to a higher probability of large wildfires associated with dry and windy Santa Ana conditions from October–January. This sequence contributed to both the 2003 and 2007 October firestorms, the November 2018 Woolsey Fire, and two major southern California winter season fires: the Thomas Fire and the Palisades and Eaton fires.

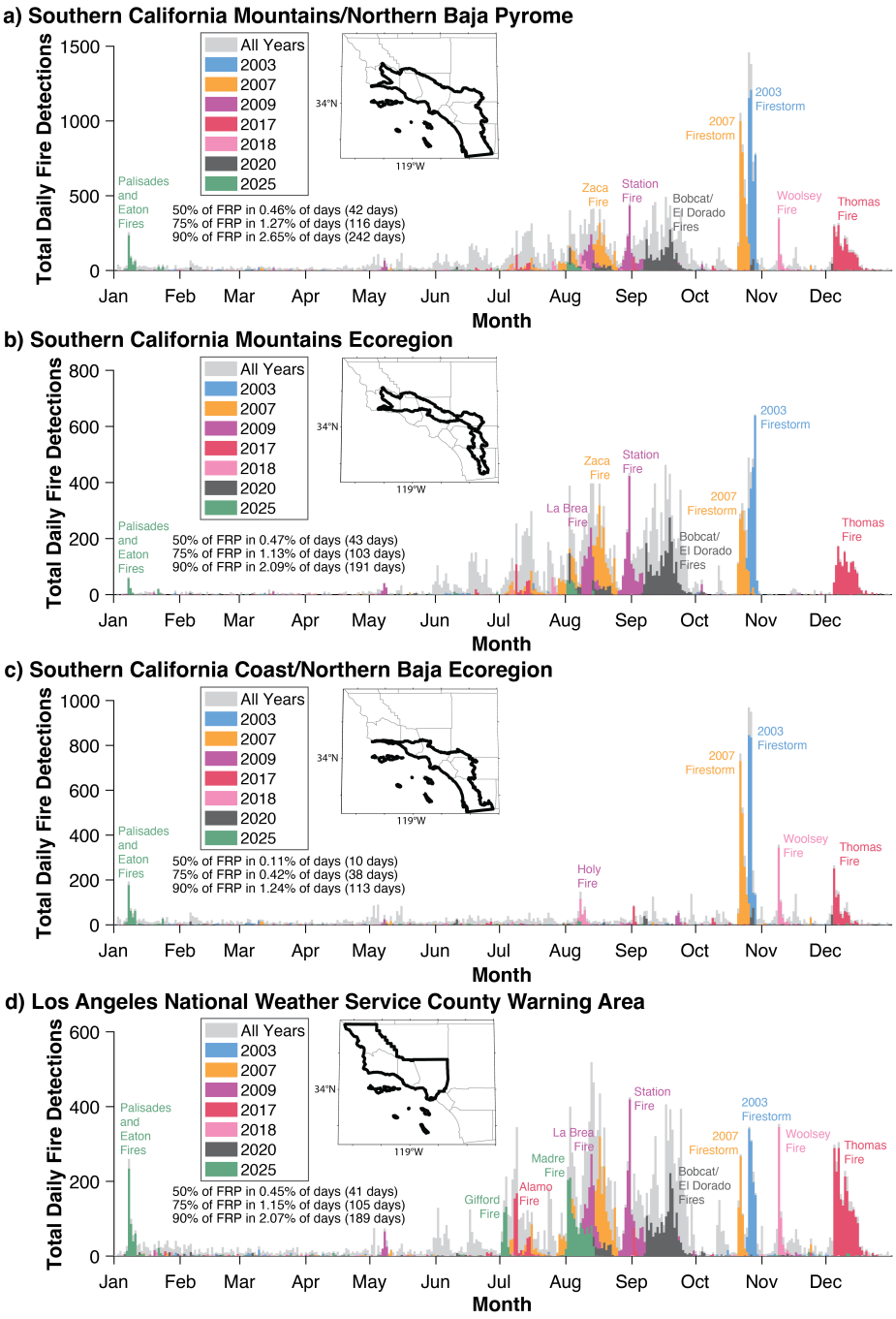

Fig. 2 (a) Pyroclimograph showing daily cumulative fire radiative power for each calendar year (2001–2025; highest three and lowest year shown) for Colusa County, California. (b) Period-of-record total daily fire detections across years (gray bars). Contributions from notable fires are colored. (c–d) As in (a–b) but for the Norman, Oklahoma (OUN) and Amarillo, Texas (AMA) NWS CWAs (2026 shown in bold red).

4.3 Towards a more complete pyroclimograph

Our motivation to extend the monthly-scale pyroclimograph proposed by Swetnam et al. (2011) is to provide a more complete picture of fire activity and the fire environment at daily timescales and merge this information with the classic pocket card style (Schlobohm 2000). The Santa Monica Mountains of Ventura and Los Angeles counties represent an ideal location to demonstrate how fire weather deviates from climatological mean conditions. Here, strong winds and low relative humidity conditions associated with occasional offshore, downslope Santa Ana winds–especially when winds occur before season-ending rainfall (Cayan et al. 2022; Guirguis et al. 2025)–produce extreme fire behavior, with 10 days contributing 90% of total FRP (Figure 3a). The number of days contributing to a given percentage of total FRP increases as the domain grows larger (Figure 2–3). However, this calculation intends to indicate whether a relatively small number of days (10 days in the Santa Monicas, or 145–242 days in the larger coastal Southern California regions; Figure 2) or a large number of days (1,906 days in the OUN–AMA region; Figure 1d) contribute to various fractions of total FRP to provide a simple metric of the frequency and intensity of fire in a region.

Merging the fire detection climatologies (Figure 3a) with an ERC climatology extends and modernizes the original pocket card (Schlobohm 2000) by including the full fire climatology for comparison with ERC percentiles calculated for days of the year and across the year (Figure 3b). The seasonal cycle of ERC indicates a peak during winter and a minima during summer; similarly, the largest range in values occurs in winter and smallest range during summer. The timing and magnitude of these ranges results from the Mediterranean climate and proximity to summer marine influences. Plotting the range-mean ERC on the ignition dates of notable recent Santa Monica fires (and two nearby high-impact fires, the 2017 Thomas Fire and 2024 Mountain Fire) show that most fire activity occurs in late fall through early winter, the exception being the Springs Fire that occurred during a late season wind event. These fires all ignited on days with above normal ERCs but none exceeded the 97^{th} percentile and many were below the annual 90^{th} percentile.

Until now, pyroclimographs have focused on the ignition component of the fire environment. Inclusion of wind, and particularly wind associated with low relative humidity, incorporates the spread component. Using the two sets of relative humidity and wind criteria for Red Flag Warnings but omitting the wind duration constraint, fire weather hours are relatively rare from May–September before reaching peak frequency during October–November (Figure 3c). They decline through the winter before a secondary peak between March–April, albeit typically when live fuel moisture is high. Just as the ERC climatology highlighted the marine stratus season, fire weather hours highlights two critical fire weather patterns affecting the Santa Monicas: the fall–winter Santa Ana season, followed by a signal of late spring Sundowner Winds that typically affect the Santa Ynez Mountains to the northwest (Hatchett et al. 2018) but can also influence the Santa Monicas.

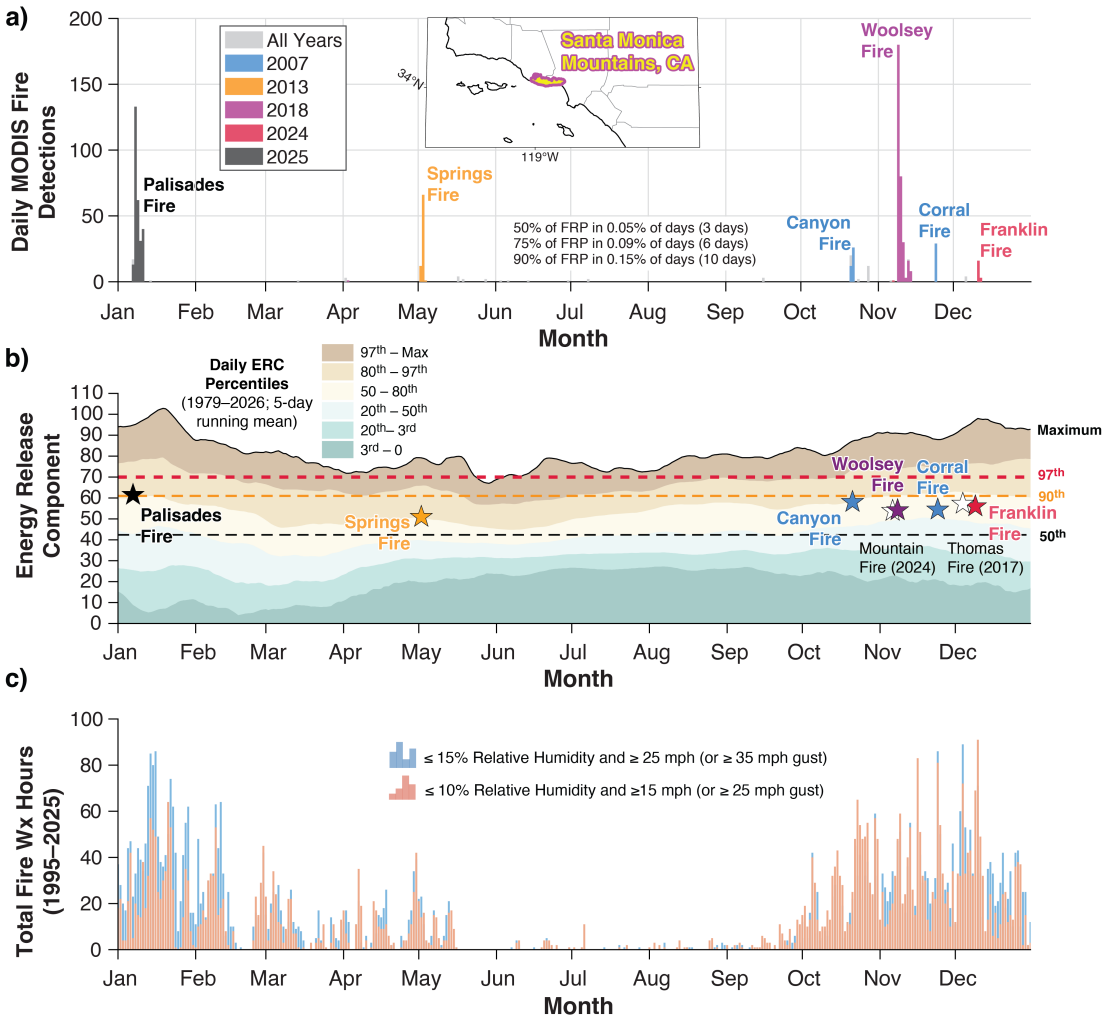

Fig. 3 Pyroclimograph showing period-of-record total daily fire detections (gray bars; left y-axis) for the Santa Monica Mountains of southern California (inset map). Contributions from notable named fires are colored by year. (b) Energy release component daily climatology with shaded regions representing percentile bins. Horizontal dashed lines represent all-time percentiles. For reference, the actual ERCs on the day of ignition for notable fires are provided; two other nearby damaging fires, the 2017 Thomas Fire and the 2024 Mountain Fire are also shown for reference. (c) Total fire daily weather hours spanning January 1995–February 2026 calculated using two sets of wind speed and relative humidity criteria for NWS LOX Red Flag Warnings at the Malibu Hills RAWS.

5 Discussion

Daily-scale pyroclimographs using satellite data provide a more temporally granular and spatially explicit perspective than historical fire perimeters that offer only

singular dates of discovery and containment (Swetnam et al. 2011) or monthly aggregations of satellite data (Giglio et al. 2009; Sablan et al. 2024). They also reveal potential prescribed burn seasonality, assuming burning occurred during satellite overflight, through the interpretation of more frequent, low FRP detections. However, integration of authoritative records of prescribed burning and wildfire are necessary to ensure correct interpretations (Sweeney et al. 2025). Assuming a correct interpretation, pyroclimographs can serve as a training tool to understand a region's satellite-era fire history, identify ideal prescribed burning timing, extract information to examine similarities and differences across regions such as fuels-driven versus wind-driven fire location and timing, and as a tool to document and contextualize the evolution of a fire season in terms of how observed fire weather deviated from normal conditions. While we focused on satellite-era fire history, longer records of fire history could be incorporated to increase the comprehensive nature of the pyroclimograph.

A limitation of our approach is that it visualizes a minimum amount of fire activity: satellites may not detect all pixels burning at all times as wildland fire progresses across the landscape. Nor can satellites identify fires that do not produce a detectable heat signature (e.g., lower-intensity below-canopy burning). False positives due to industry or sun glint may cause some overestimation of counts and require additional investigation. An upcoming challenge for data continuity will be to merge MODIS and the Visible Infrared Imaging Radiometer Suite (VIIRS) detection climatologies as the MODIS mission approaches decommissioning and VIIRS becomes the primary fire detection data source.

Reporting climatological mean conditions likely underestimates the potential for fire activity, which may only require several hours to yield favorable conditions for ignition and extreme fire behavior that presents resistance to control. It also prevents clear identification of the frequency, timing, magnitude, and duration of anomalous conditions favoring wildland fire. Because many fire-prone regions are characterized by variability of environmental conditions across intraseasonal (winter wet spells versus mid-winter dry spells followed by dry and windy Santa Anas), interseasonal (fall and winter Santa Ana events versus summer drought or convective storms), and interannual timescales, inclusion of fire weather variability, as done here using ERCs and fire weather hours, only estimates the first-order potential for fire. Identifying the specific conditions associated with burning will aid in the identification of the atmospheric processes driving them, improving their predictability and thus community preparation. Subsequent iterations of pyroclimographs will include local conditions extracted on the day (or hour) of burning to better assess their role during rapid fire spread or high FRP events and how conditions influence burn severity (Orland et al. 2025).

6 Closing Remarks

We revisited the concept of pyroclimographs as simple visualizations leveraging satellite fire detections to demonstrate a facet of pyrogeography: the "where of fire when" to understand "the why of fire." Providing a daily perspective of wildland fire activity, pyroclimographs contextualize a region's satellite-era fire history and support the interpretation of past fire events, especially when complemented with fire environment

data. With no additional information, a pyroclimograph indicates when fire activity has not (yet) been observed, when fire activity may be common but less with lower FRP (potential prescribed burning) versus infrequent but higher FRP (potential wildfire). By including fire environment-related data and its variability, a picture emerges of why certain seasons typically do or do not have increased fire activity and why anomalous events occurred. The simplicity of these visualizations is intentional; it is our aim that they can be used not just for scientific or tracking purposes but also for educational and training purposes for anyone willing to interpret a time series for the appropriate domain.

Acknowledgements. Benjamin Hatchett was supported by a NOAA cooperative agreement for the Cooperative Institute for Research in the Atmosphere (NA24OARX432C0007), the Bipartisan Infrastructure Law (BIL) Provision 5, Fire 2 (NA23OAR40504161), the Disaster Relief Supplemental Appropriations Act (NA23OAR4050133D). Alan Rhoades was funded by the Office of Science, Office of Biological and Environmental Research of the U.S. Department of Energy Regional and Global Model Analysis (RGMA) and MultiSector Dynamics (MSD) Program Areas "the Calibrated and Systematic Characterization, Attribution and Detection of Extremes (CASCADE)" Science Focus Area (DE-AC02-05CH11231) and the "An Integrated Evaluation of the Simulated Hydroclimate System of the Continental US" (HyperFACETS) project (DE-SC0016605). The statements, findings, conclusions, and recommendations are those of the authors and do not reflect the views of NOAA, the U.S. Department of Commerce, the USFS, NASA, or the U.S. Department of Energy.

References

Abatzoglou, J.T. 2013. Development of gridded surface meteorological data for ecological applications and modelling. *International Journal of Climatology 33*(1): 121–131. https://doi.org/https://doi.org/10.1002/joc.3413 .

Al-Yaari, A., T. Condom, C. Junquas, A. Rabatel, V. Ramseyer, J.E. Sicart, M. Masiokas, S. Cauvy-Fraunié, and O. Dangles. 2023. Climate variability and glacier evolution at selected sites across the world: Past trends and future projections. *Earth's Future 11*(10): e2023EF003618. https://doi.org/https://doi.org/10.1029/2023EF003618 .

Balch, J.K., V. Iglesias, A.L. Mahood, M.C. Cook, C. Amaral, A. DeCastro, S. Leyk, T.L. McIntosh, R.C. Nagy, L.S. Denis, T. Tuff, E. Verleye, A.P. Williams, and C.A. Kolden. 2024. The fastest-growing and most destructive fires in the US (2001 to 2020). *Science 386*(6720): 425–431. https://doi.org/10.1126/science.adk5737. https://www.science.org/doi/pdf/10.1126/science.adk5737 .

California Annual Operating Plan. 2025. California Annual Operating Plan 2025. https://www.weather.gov/media/wrh/cafw/2025_CA_FIRE_AOP.pdf.

Cayan, D.R., L.L. DeHaan, A. Gershunov, J. Guzman-Morales, J.E. Keeley, J. Mumford, and A.D. Syphard. 2022, 10. Autumn precipitation: the competition with

Santa Ana winds in determining fire outcomes in southern California. *International Journal of Wildland Fire 31*(11): 1056–1067. https://doi.org/10.1071/WF22065 .

Giglio, L., T. Loboda, D.P. Roy, B. Quayle, and C.O. Justice. 2009. An active-fire based burned area mapping algorithm for the modis sensor. *Remote Sensing of Environment 113*(2): 408–420. https://doi.org/https://doi.org/10.1016/j.rse.2008.10.006 .

Giglio, L., W. Schroeder, and C.O. Justice. 2016. The collection 6 modis active fire detection algorithm and fire products. *Remote Sensing of Environment* 178: 31–41. https://doi.org/https://doi.org/10.1016/j.rse.2016.02.054 .

Guirguis, K., B. Hatchett, R. Clemesha, R. Aguilera, A. Gershunov, I. Campbell, D. Cayan, and M. Merrifield. 2025, Dec. Compound atmospheric drivers of the catastrophic 2025 Los Angeles urban firestorm. *npj Natural Hazards 2*(1): 103. https://doi.org/10.1038/s44304-025-00155-7 .

Hantson, S., N. Andela, M.L. Goulden, and J.T. Randerson. 2022, May. Human-ignited fires result in more extreme fire behavior and ecosystem impacts. *Nature Communications 13*(1): 2717. https://doi.org/10.1038/s41467-022-30030-2 .

Hatchett, B.J., C.M. Smith, N.J. Nauslar, and M.L. Kaplan. 2018. Brief Communication: Synoptic-scale differences between Sundowner and Santa Ana wind regimes in the Santa Ynez Mountains, California. *Natural Hazards and Earth System Sciences 18*(2): 419–427. https://doi.org/10.5194/nhess-18-419-2018 .

Hatchett, B.J. and E.M. Wells. 2026. Good fire weather. *Bulletin of the American Meteorological Society*. https://doi.org/https://doi.org/10.1175/BAMS-D-25-0209.1 .

Lasantha, V., T. Oki, and D. Tokuda. 2022. Data-Driven versus Köppen–Geiger systems of climate classification. *Advances in Meteorology 2022*(1): 3581299. https://doi.org/https://doi.org/10.1155/2022/3581299 .

Omernik, J.M. and G.E. Griffith. 2014, Dec. Ecoregions of the conterminous United States: evolution of a hierarchical spatial framework. *Environmental Management 54*(6): 1249–1266. https://doi.org/10.1007/s00267-014-0364-1 .

Orland, E., T.D. McCabe, Y. Chen, R.C. Scholten, Z. Becker, R.A. Loehman, J.T. Randerson, S.R. Coffield, T. Liu, A.N. Shiklomanov, K. Nelson, B. Peterson, M.B. Follette-Cook, and D.C. Morton. 2025, Oct. Near real-time indicators of burn severity in the western U.S. from active fire tracking. *Fire Ecology 21*(1): 55. https://doi.org/10.1186/s42408-025-00407-x .

Sablan, O., B. Ford, E. Gargulinski, M.S. Hammer, G. Henery, S. Kondragunta, R.V. Martin, Z. Rosen, K. Slater, A. van Donkelaar, H. Zhang, A.J. Soja, S. Magzamen, J.R. Pierce, and E.V. Fischer. 2024. Quantifying prescribed-fire smoke

exposure using low-cost sensors and satellites: Springtime burning in eastern kansas. *GeoHealth 8*(4): e2023GH000982. https://doi.org/https://doi.org/10.1029/2023GH000982 .

Schlobohm, P. 2000. Application of the fire danger pocket card for firefighter safety. https://wildfireweb-prod-media-bucket.s3.us-gov-west-1.amazonaws.com/s3fs-public/2022-11/pc_apply.pdf.

Short, K.C., I.C. Grenfell, K.L. Riley, and K.C. Vogler. 2020. Pyromes of the conterminous United States. Fort Collins, CO: Forest Service Research Data Archive.

Snethlage, M.A., J. Geschke, A. Ranipeta, W. Jetz, N.G. Yoccoz, C. Körner, E.M. Spehn, M. Fischer, and D. Urbach. 2022, Apr. A hierarchical inventory of the world's mountains for global comparative mountain science. *Scientific Data 9*(1): 149. https://doi.org/10.1038/s41597-022-01256-y .

Sweeney, B., W.M. Jolly, P.H. Freeborn, and C. Ochocki. 2025. ClassiFiRxe: a data-driven tool to support prescribed fire planning and implementation. *Preprint submitted to SSRN*. https://doi.org/http://dx.doi.org/10.2139/ssrn.5846214 .

Swetnam, T.W., D.A. Falk, E.K. Sutherland, P.M. Brown, and T.J. Brown. 2011. Final report, 2011: Fire and climate synthesis (facs) project, jfsp 09-2-01-10. https://www.researchgate.net/publication/292610619_Final_Report_2011_Fire_and_Climate_Synthesis_FACS_Project_JFSP_09-2-01-10.

The MathWorks Inc. 2024. Matlab version: 24.1.0 (r2024a).

Worsnop, R.P., A. Hoell, B.J. Hatchett, T.B. Chapman, M.L. Breeden, Z. Zach Tolby, K.C. Short, and M. Hobbins. 2026. Characterizing windows of opportunity for prescribed pile and broadcast burning in Northern California. *Fire Ecology*. https://doi.org/10.1186/s42408-026-00492-6 .